ISSN (Print) : 0974-6846
Indian Journal of Science and Technology, *Vol 8(30), DOI: 10.17485/ijst/2015/v8i30/85942, November 2015* ISSN (Online) : 0974-5645

Active Vibration Control to Attenuate Hand-arm Vibration from Orbital Sander: A Mathematical Model Approach

Ahmad Zhafran Ahmad Mazlan* and Zaidi Mohd Ripin

School of Mechanical Engineering, Universiti Sains Malaysia, 14300 Nibong Tebal, Pulau Pinang, Malaysia; zulryan_85@yahoo.com

Abstract

Prolonged exposure to the orbital sander with high vibration level can lead to the Hand-arm Vibration Syndrome (HAVs). In order to attenuate the vibration when using the orbital sander, dynamic analysis of the orbital sander is carried out using coupled orbital sander-hand-arm model subjected to the Active Vibration Control (AVC). The orbital sander is modelled as a three-degree-of-freedom system where the values of the dynamic mass, stiffness and damping are derived from the experimental modal analysis and the single-degree-of-freedom of Reynolds and Soedel model is chosen to represent the hand-arm system. Various control schemes are applied in the AVC system including Proportional-Derivative (PD) and Active Force Control (AFC) techniques. Two disturbances are created for the system where the first disturbance is measured from the orbital sander operating condition and the second disturbance is modelled as a sine wave to test the robustness of the control schemes. The simulation result shows that the control scheme with AFC produced a superior result compared to the classical PD controller, even though under the influence of external disturbance with a vibration reduction of 99% and 88%, respectively.

Keywords: Active Vibration Control, AFC Control, Orbital Sander, PD Control

1. Introduction

Orbital sander is widely used in the preparation of surface for further coating, to achieve the required surface roughness and to remove rust. It is widely used in the automotive repair, composite manufacturing and in fabrication of metallic panels product. Since the application of orbital sander is highly irregular and unplanned such as in the application of correction of pressed panels, its use is mainly manual since automation is not cost effective. However, the use of orbital sander will expose the user to the hand-arm vibration and if uncontrolled can lead to the health hazard associated with Hand-arm Vibration syndrome (HAVs)[1].

There are several ways of reducing the vibration level transmitted to the hand. The best method is to remove all the unbalanced force in the system. For example, power tool manufacturer has managed to dynamically balance the motor of the electric jigsaw which resulted in 40% reduction of vibration[2]. Some manufacturers have resorted to create counter rotating head of the sander to balance the orbital motion and claimed that the design is able to reduce the vibration level of the sander. For some reason, most major orbital sanders did not have two counter rotating head due to the complex design of the housing and the increased number of components which increases the overall cost of the sander. As such for the aftermarket demand, the remaining solution is to go for the passive or Active Vibration Control (AVC) technologies. For the passive way, this can be achieved by inserting isolator between the hand and the sander. The isolator can be in the form of anti-vibration glove[3] or simple insertion

**Author for correspondence*

of elastomeric pad[4]. In general, anti-vibration gloves will limit the dexterity of the fingers and elastomeric pad lack the positive feeling of control when the palm is grasping the orbital sander. Another possibility is the use of Dynamic Vibration Absorber (DVA)[5] which can be tuned to match the operating frequency. However, this has problem when the sander is loaded since the speed of the sander will be reduced and the tuning effectiveness diminished.

Another potentially available solution is the application of an active vibration control, where the actuator can be used to supply equal but opposite signal to the sander at one end and with the other end connected to the base of the pad. This possibility is explored in this paper where the conceptual design of an AVC pad is applied to the orbital sander and the effectiveness is calculated. The main objective of this research is to develop the dynamic model of the hand-arm coupled with the orbital sander and to design the AVC with variable control techniques based on the existing hardware and also modeling the system to measure its efficacy.

2. Methodology

2.1 System Identification

The orbital sander system identification is carried out using Experimental Modal Analysis (EMA). The result of Frequency Response Function (FRF) from the EMA can be used to determine the dynamic mass, damping and stiffness for the creation of orbital sander model. In this work, the experimental modal analysis is carried out for the orbital sander with a no-load speed of 12000 rpm using LMS Test Lab software. This consists of geometry modelling and impact testing experiment. Figure 1 shows the geometry model of the orbital sander in LMS software and the impact testing set-up for the orbital sander in a free-free condition. A total of 72 nodes are defined to create the actual shape of the orbital sander.

2.2 Sensor and Actuator Locations

Sensor and actuator location in general is based on the vibration transmission path. Since the orbital sander size is small, the location of the actuator is limited at the handle, where the AVC pad is connected and the piezo actuator is inserted between the pad and the handle. The sensor in this case will measure the angle of the rotating shaft since the force is related to the location of the off-center axis of the pad cam relative to the axis of the motor. To determine the axis and location of the handle that contribute most vibration to the hand, an input spectrum testing is performed using iMC device software.

Figure 2 shows the measurement set-up for the input spectrum measurement. A tri-axial accelerometer is mounted on top of the orbital sander to capture the acceleration in the three axes (x, y and z-axis) during polishing

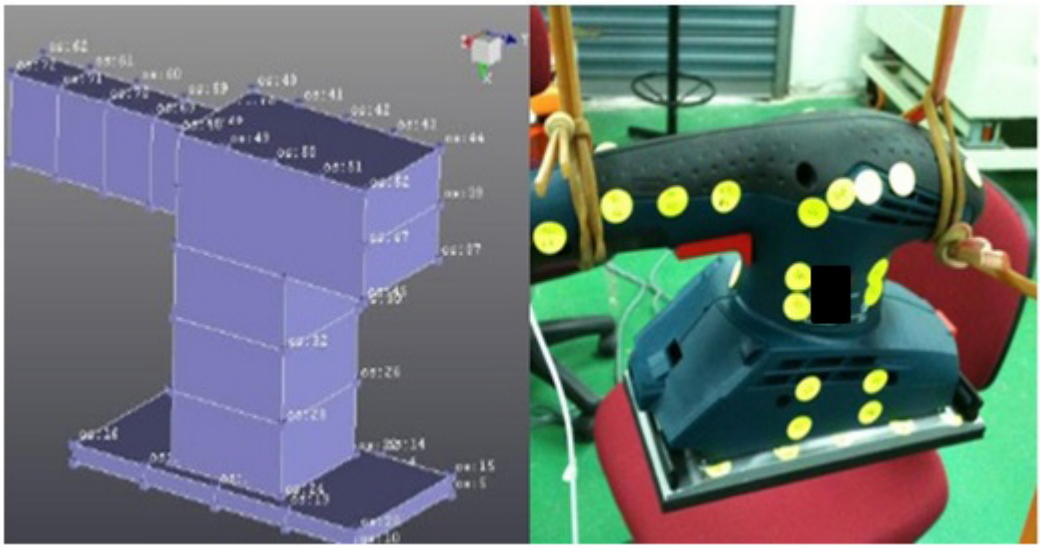

(a) (b)

Figure 1. Experimental modal analysis (a) Geometry modeling. (b) Impact testing.

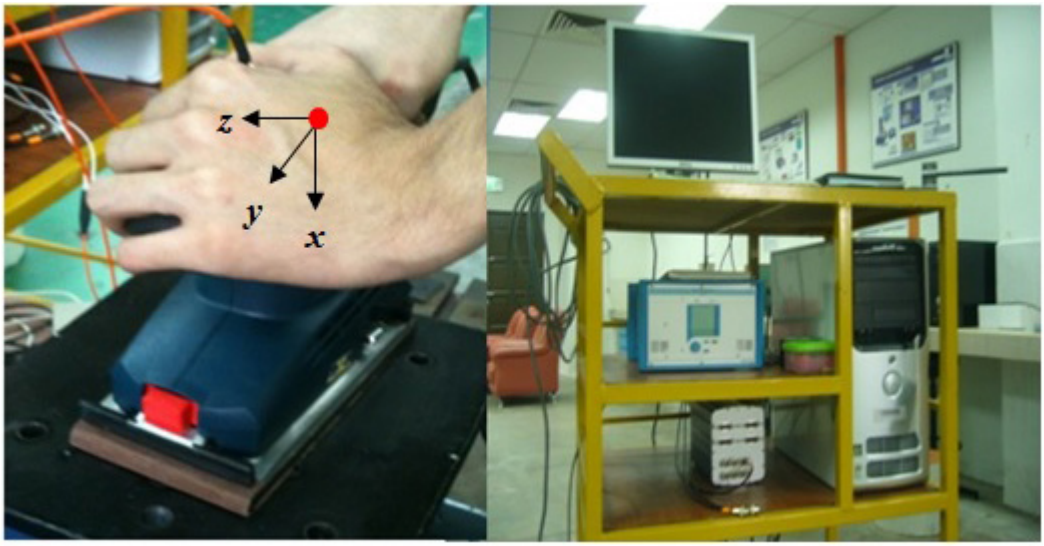

(a) (b)

Figure 2 Input spectrum measurement set-up using iMC devices.

work on the mild steel plate, which mounted on top of the dynamometer to measure the push force. The orbital sander is operated with an approximation nominal push force of 30 N on the mild steel plate as shown in Figure 2.

2.3 Actuator Selection

There are many types of actuators available in the market to use in the AVC application, such as piezoelectric actuator and MR damper[6]. For this study, an actuator selection is based on the available piezoelectric actuator[7] which can be fitted in between the pad and the handle of the orbital sander. In this case the desired dimension is 10 mm diameter or smaller with dynamic force capacity to match the force applied on the orbital sander and can vary with the applied load on the handle. At this stage, the piezoelectric actuator is assumed to be linear and the equation of the piezoelectric actuator can be represented as:

$$F_a = k_a z_a \tag{1}$$

Where, k_a is the piezo actuator stiffness, z_a is the stroke and F_a is the actuator force. Since the orbital sander is hold at the palm of the hand, the relative motion between the palm and the sander is creating shear deformation of the palm. Based on this, it is recommended that the actuator used is a shear piezoelectric actuator, which can generate high force. In this case, a bi-axial direction of the shear allows for the compensation of motion in the sanding plane. For this design a minimum of one shear actuator is targeted due to cost reason.

2.4 System Modelling and Control Algorithm Development

For the system modelling, an orbital sander is represented as a three-degree-of-freedom system which subjected to the measured input spectrum force F_i. A Reynolds and Soedel[8] single-degree-of-freedom model is selected to represent the hand-arm system and to characterize the dynamic response of human hand-arm under vibration. This model matched the DPMI under specific condition when the hand is gripping a cylinder-type handle, which consider valid within 20~500 Hz with a push force less or equal to 50 N[9]. Figure 3 shows the coupled orbital sander hand-arm model and the equation of motion of the system can be written as:

$$m_1\ddot{z}_1 + (c_1 + c_2)\dot{z}_1 - c_2\dot{z}_2 + (k_1 + k_2)z_1 - k_2 z_2 = F_i + F_e \tag{2}$$

$$\begin{aligned} m_2\ddot{z}_2 - c_2\dot{z}_1 + (c_2 + c_3)\dot{z}_2 - c_3\dot{z}_3 - k_2 z_1 \\ +(k_2 + k_3)z_2 - k_3 z_3 = 0 \end{aligned} \tag{3}$$

$$\begin{aligned} m_3\ddot{z}_3 - c_3\dot{z}_2 + (c_3 + c_h)\dot{z}_3 - c_h\dot{z}_h - k_3 z_2 + (k_3 + k_h)z_3 \\ -k_h z_h = -F_a * \end{aligned} \tag{4}$$

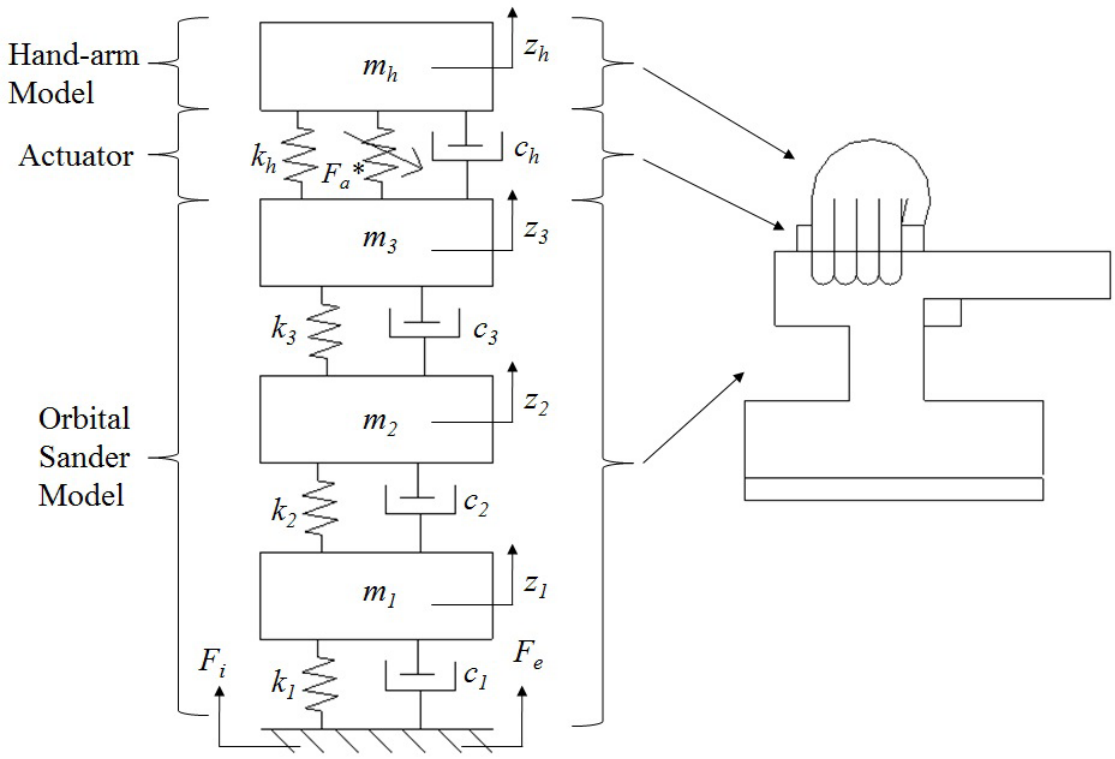

Figure 3. Coupled orbital sander-hand-arm model.

$$m_h\ddot{z}_h - c_h\dot{z}_3 + c_h\dot{z}_h - k_h z_3 + k_h z_h = F_a * \quad (5)$$

Where, *Fi* and *Fe* are the internal and external disturbance forces, *mh*, *ch* and *kh* are the dynamic mass, damping and stiffness of the hand-arm model[8], *mn*, *cn* and *kn* are the dynamic mass, damping and stiffness of the orbital sander, which the subscript of *n* = 1, 2 and 3 represented the degree-of-freedom which adequately represent the orbital sander.

In this work, two types of controllers are developed which is Proportional-derivative (PD)[10] and Active Force Control (AFC) controllers[11]. The actuating force *Fa** of Equations (4) and (5) that generated by each controller are shown as:

a) AVC with PD controller

$$F_{a1} * = k_a(\kappa_p e(t) + \kappa_D de(t)/dt) \quad (6)$$

b) AVC with PD+AFC controller

$$F_{a2} * = k_a((\kappa_p e(t) + \kappa_D de(t)/dt) + (F_a - M * \ddot{z}_3)1/k_a) \quad (7)$$

Where, K_P and K_D are the proportional and derivative constants and M* is the estimated mass. The AVC system block diagram with PD and AFC controllers are shown in Figure 4.

3. Results and Discussion

3.1 Experimental Results and Model Validation

Figure 5 shows the acceleration frequency response of the orbital sander in three axes, with giving push force of 30 N on the dynamometer.

From the figure, the vibration level in *z*-axis is 43.35 m/s^2, which is the highest vibration level compared to the *x* and *y*-axes of the orbital sander. It also observed that the first peak of the acceleration level is reduced to 175 Hz approximately compared to actual motor with a no load speed of 200 Hz, due to the resistance of the work-piece. Since the result of vibration is prior and more significant in *z*-axis direction, the attenuation of vibration should be focused in this direction.

From the result of Figure 5, an experimental modal analysis is focused in *z*-axis direction which

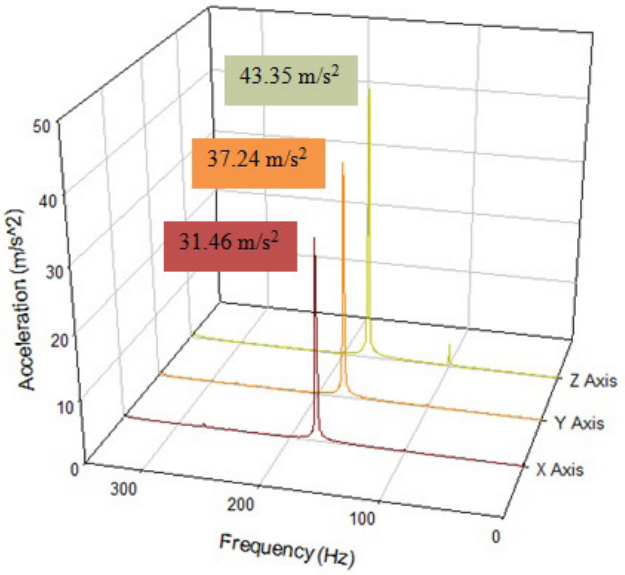

Figure 5. Input spectrum of the orbital sander in three axes.

corresponding to the dominant vibration axis when operating the orbital sander. Table 1 represented the first three modes with the dynamic mass, damping and stiffness values for frequency below 350 Hz in *z*-axis direction. Since the operating frequency of orbital sander is 175 Hz, only modes between frequencies of 50~350 Hz are being considered. All the modes are generated using the LMS Test lab software and then been scaled to the unit modal masses and normalized to the amplitude.

Table 1. Dynamic mass, damping and stiffness for the first three modes below 350 Hz of the orbital sander

Modes	Frequency (Hz)	Dynamic mass (kg)	Dynamic damping (kg/s)	Dynamic stiffness (N/m)
1	98	0.481	298.7	1.856 x 10^5
2	154	0.446	433.8	4.216 x 10^5
3	300	0.179	338.9	6.406 x 10^5

Before modeling an orbital sander, the values of the dynamic mass, damping and stiffness must be verify by obtaining an equivalent FRF between the experiment and model. The FRF validation result between the experiment and model of the orbital sander is shown in Figure 6.

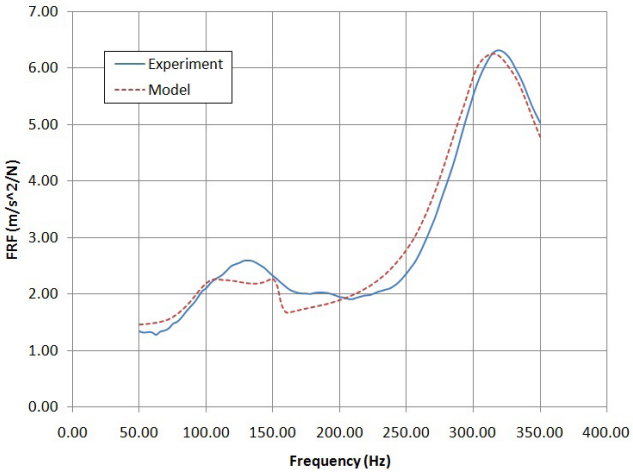

Figure 6. Experimental and model FRF of the orbital sander.

From the figure, the FRF trend for both experiment and model of the orbital sander are quite similar within the frequency range of 50~350 Hz, with a very small error of 1.45% between them. Therefore, the values of the dynamic mass, damping and stiffness that have been calculated can be represented the orbital sander.

3.2 Performance of Orbital Sander with Various Control Schemes

In this section, three different mathematical models; passive, active with PD controller and active with PD + AFC are designed in Matlab and Simulink software, followed by creating the disturbances model and finally combined with the hand-arm model as a full AVC system diagram. The active system is specifically modelled with a feedback control embedded to the system. In this simulation, two types of disturbances are introduced to the system. The first disturbance F_i is an internal disturbance which taken from the input spectrum measurement when operating the orbital sander using the sand paper to carry out sanding work on the mild steel plate. This disturbance is introduced to the system during the tuning of the control schemes. The second disturbance F_e is modelled as a sine wave with variable input forces. This disturbance is introduced to the system after the tuning process, in order to examine the robustness of the control schemes.

The process of controller tuning is an essential task to make sure that the controller can produces the desirable results. The result of PD and AFC controllers tuning are shown in Figure 7(a) and 7(b), respectively.

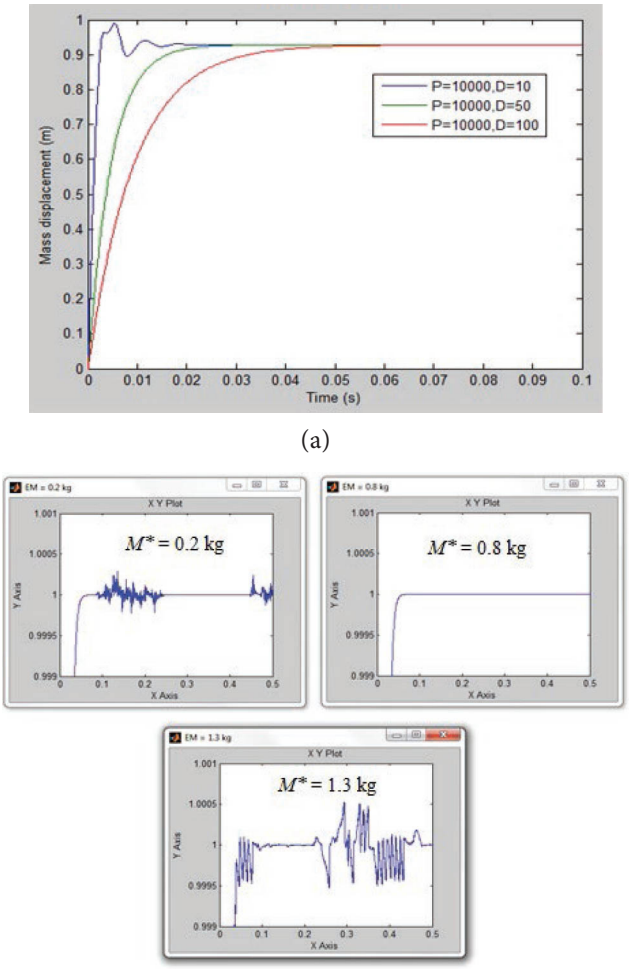

Figure 7. (a) PD and (b) AFC controllers tuning.

In this case, Crude Approximation (CA)[11] tuning method is chosen and a constant value of one is used as a reference step-input signal for the case of initial condition. This value is later changed to zero for the complete AVC system, since we want to eliminate any undesirable vibration that could disturb worker's comfort while using the orbital sander. A number of combinations for K_P, K_I and K_D values have been investigated and the best combination is obtained as K_P = 10,000 and K_D = 50, as shown in Figure 7(a). Only P and D are used as a controller instead of P, I, and D because the value of K_I doesn't contribute to suppress the vibration for this model.

For an AFC controller, the same CA method is used to determine appropriated estimated mass value M* and the obtained value is M* = 0.8 kg, as shown in Figure 7(b). The piezoelectric actuator stiffness k_a = 350 N/m is chosen in this model since the value is suitable for the hand-held power tools that operate within the frequency range below 500 Hz[11].

Figure 8 shows the time series result of acceleration between passive, PD and PD + AFCCA models without and with an external disturbance for the orbital sander.

From the figure, it is clear that the PD + AFCCA scheme gives the best result with 97% of vibration suppression compared to the PD controller with 91%. For the case of presence of an external disturbance to the system, PD + AFCCA proved that the scheme is robust with good vibration suppression while PD controller has the vibration effect because of the external disturbance.

3.3 Performance of Coupled Orbital Sander-hand-arm Model with External Disturbances

The hand-arm model is designed in the Matlab and Simulink software to observe the effect of vibration transmitted to the hand-arm system from the orbital sander. This model is later combined with previous three models of the orbital sander to observe the vibration effect to the controller schemes and the hand-arm system. The forces generated by the result of acceleration from the orbital sander for both conditions; with and without the external disturbances, are used as an input disturbance to the hand-arm system. Figure 9 shows the time series result of acceleration of the coupled orbital sander-hand-arm system between passive, PD and PD + AFCCA models.

From the figure, it is observed that the PD + AFCCA scheme has suppressed about 99% of vibration from the orbital sander to the hand-arm system while the PD controller has suppressed about 88% of vibration from the orbital sander. For the case with an external disturbance, PD controller increased the transmitted vibration to the hand-arm system while PD + AFCCA can maintain as a robust control scheme although under the influence of an external disturbance.

4. Conclusion

In this research, the main target to build a dynamic model of the hand-arm coupled with the orbital sander

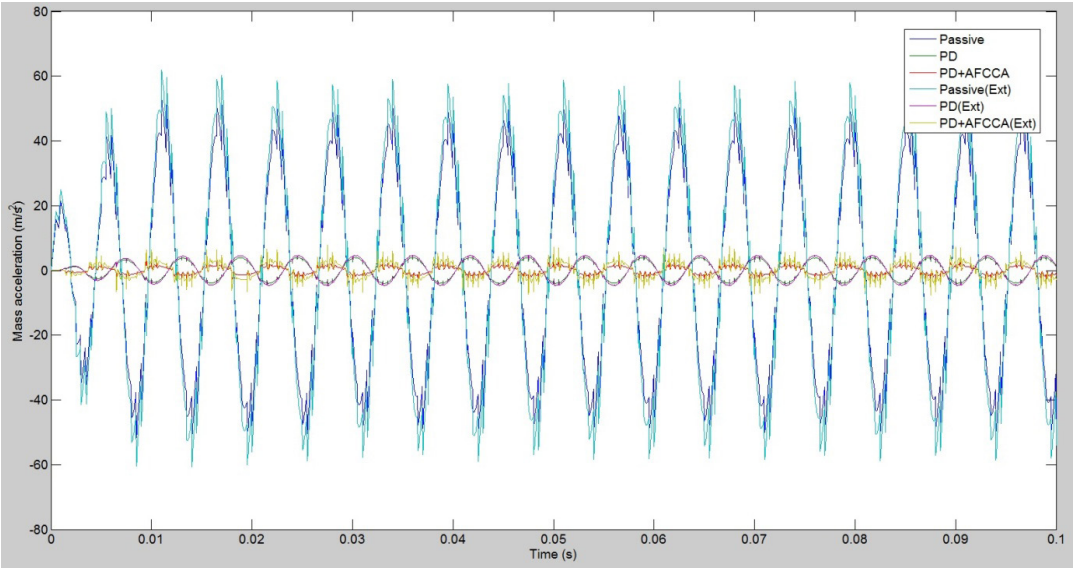

Figure 8. Acceleration comparison between passive, PD and PD + AFCCA of the orbital sander model.

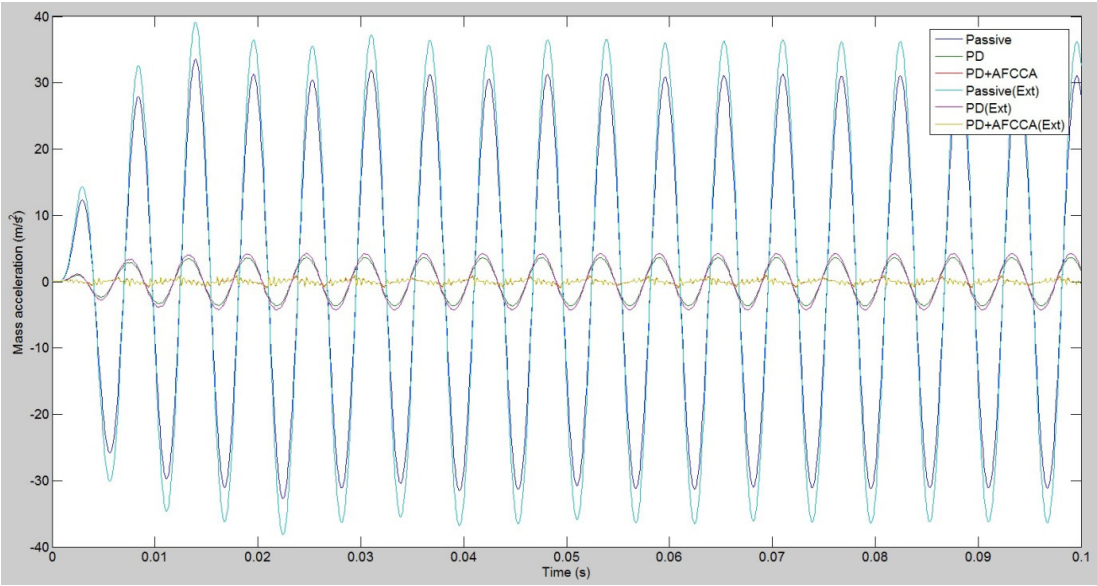

Figure 9. Acceleration comparison between passive, PD and PD + AFCCA of the coupled orbital sander-hand-arm model.

based on the existing hardware is successfully developed. The conceptual design of an AVC pad can suppress the undesirable vibration generated by the orbital sander and can eliminate the vibration transmitted to the hand-arm system using an AFC technique. This study also proved that the AFC controller can produce superior result compared to the PD controller, even though under the influence of external disturbances. Further investigation by developing the experimental rig can be performed to prove the reliability of the model developed here.

5. Acknowledgement

The authors would like to thank Universiti Sains Malaysia for funding this work.

6. References

1. Mansfield NJ. Human response to vibration. CRC Press LLC. 2005. p.77–96.
2. Makita U.S.A. Inc. Makita 4350 FCT top handle jigsaw with LED light; 2015. Available from: http://www.makita.com/en-us/Modules/Tools/ToolDetails.aspx?ID=24060
3. Dong RG, McDowell, McDowell DE. Welcome, Biodynamic response at the palm of the human hand subjected to a random vibration. Industrial Health. 2005; 43:241–255.
4. Ko YH. Investigation of elastomeric pad attenuation of hand-transmitted vibration [MSc Thesis]. Universiti Sains Malaysia; 2008.
5. Ko YH, Lee XM, Ripin ZM. Tuned vibration absorber for suppression of hand-arm vibration in electric grass trimmer. International Journal of Industrial Ergonomics. 2011; 41:494–508.
6. Ekkachai K, Tungpimolrut K, Nilkhamhang I. A novel approach to model magneto-rheological dampers using EHM with a feed-forward neural network. Science Asia. 2012; 38:386–93.
7. Physik Instruments (PI), Fundamental of piezoelectric actuators. 2009; 2:177–91.
8. Reynolds DD, Soedel W. Dynamic response of the hand-arm system to a sinusoidal input. Journal of Sound and Vibration. 1972; 21:339–53.
9. Rakheja S, Wu JZ, Dong RG, Schopper AW. A comparison of biodynamic models of the human hand-arm system for application to hand-held power tools. Journal of Sound and Vibration. 2002; 249:55–82.
10. Kittisupakorn P, Hussain MA, Siripun N, Daosud W, Kaewpradit P. Use of globally linearizing control with extended kalman filter for pH control of a wastewater treatment process. Science Asia. 2002; 28:365–82.
11. Hassan MF, Mailah M, Junid R, Alang NA. Vibration suppression of a handheld tool using intelligent Active Force Control (AFC). Proceedings of the World Congress on Engineering (WCE), London. 2010; 2.